DESIGN, TESTING, AND FIELD EXPERIENCE OF A HIGH-PRESSURE NATURAL GAS REINJECTION COMPRESSOR

by

Norbert G. Wagner

Demag Delaval Turbomachinery

Head, Mechanical R&D Group

Duisburg, Germany

Frits M. de Jongh

Demag Delaval Turbomachinery

Research and Development Manager

Hengelo, The Netherlands

and

Robert Moffat

Technical Integrity Manager

Pierce Production Company

Aberdeen, Scotland

Norbert G. Wagner is Head of the Mechanical R&D group of Demag Delaval Turbomachinery, in Duisburg, Germany. In this capacity, he is responsible for the mechanical developments and for providing technical support in rotordynamics and stress analysis. During his more than 19 years with this company, Mr. Wagner has given special attention to rotordynamics of high-pressure applications and to active magnetic bearings. He has conducted extensive analytical and experimental investigations on the effect of labyrinth seals on rotor stability and he has authored several papers on this issue.

Mr. Wagner received his Diplom degree from the University of Duisburg (1981).

Frits M. de Jongh is Research and Development Manager for Demag Delaval Turbomachinery B.V., in Hengelo, the Netherlands. He has 20 years of diversified experience in the fields of testing rotating machinery, solving vibration problems, rotordynamic research, and compressor stage performance investigations. He joined the company's R&D department in 1989, where he is currently responsible for the coordination and execution of all research and development activities at the Hengelo division.

Mr. de Jongh received a degree in Mechanical Engineering (1980) from the Dordrecht Institute of Technology. He has authored and coauthored several technical turbomachinery papers.

Robert Moffat is Technical Integrity Manager for Pierce Production Company (PPC), in Aberdeen, Scotland. PPC is a special purpose company created to operate the floating production storage and offloading (FPSO) vessel, Berge Hugin. This vessel is a converted multipurpose shuttle tanker, which is operated in the Enterprise Oil licensed Pierce Oil Field, in the United Kingdom Sector of the North Sea.

Mr. Moffat was originally seconded to the project from Aker Oil and Gas Technology, in January 1998. He was responsible for the development and implementation of all technical system's procedures and routines to ensure a seamless transition from project to operation phase. Mr. Moffat is responsible for the technical integrity of the FPSO, and the safe and efficient performance of all plant and equipment onboard. He has 22 years' experience in the offshore oil and gas industry.

ABSTRACT

This paper explains the design and testing of a high-pressure centrifugal compressor. It also covers commissioning and field experience. Important issues for high-pressure compressors are highlighted in the paper in general terms and for a specific design. Included are the mechanical impeller design, seal clearance control, and rotor stability.

The impeller integrity is ensured by means of finite element analysis and supported by experimental modal analysis. During full load testing, a unique measurement was also carried out in order to verify the relative rotor displacement in the balance drum labyrinth under transient conditions. Special consideration is given to the verification of analytical rotor stability predictions, which is of major importance for high-pressure applications. The forces

originating from the labyrinth seals tend to destabilize the rotor. The rotordynamic analysis is presented for a 418 bar (6061 psi) natural gas reinjection compressor. The predictions from this analysis were verified during an ASME/PTC-10 Class I (1997) test on the test stand. The compressor was tested with and without labyrinth swirl brakes, respectively, and the unit could be brought purposefully to the stability threshold by variation of different parameters. Testing according to the design with swirl brakes installed resulted in reliable, trouble-free operation. This has been confirmed by actual field data from a floating production, storage, and offloading (FPSO) vessel in the North Sea.

INTRODUCTION

The requirements relating to the operational reliability and safety of centrifugal compressors are particularly high in the offshore field. Since these qualities are determined essentially by the design of the rotating parts, it is important to have a good knowledge of the designing of these parts and to be able to adapt the design process to the ever more stringent requirements. This applies above all to the shaft end seals, the impellers, and the rotordynamic design.

Since the costs resulting from failure of a compressor are very high in this field of application, the operational reliability is as a rule valued higher than the efficiency. However, the safety margins are being reconsidered continuously due to the attempts to achieve the lowest possible investment costs and also to the growing stringency of environmental regulations and the rising energy costs. In any case, it is necessary to avoid the efficiency-related disadvantages resulting from an overly conservative design.

Rotordynamics are of major importance in view of the fact that several aerodynamic parameters such as the hub-to-tip ratio, the number of stages, and the inline or back-to-back arrangement of the stages has an important influence on the rotordynamics. There are several possibilities for the rotordynamic design aimed at the achievement of a robust and reliable operating behavior. The authors' approach involves the systematic and detailed analysis of all components that have an influence on the rotordynamic behavior. This enables a modeling to be implemented that shows a high targeting accuracy and avoids the disadvantages of superfluous measures. Testing of the vibration behavior of completed machines at the test stand is utilized for validating the employed models.

GENERAL DESIGN ASPECTS RELATING TO HIGH-PRESSURE COMPRESSORS

Overall Design

A typical high-pressure compressor casing is of a barrel design and is made of a single piece cup forging, as shown in Figure 1. The gas inlet and outlet nozzles are flanged directly to the compressor casing. The end cover is bolted to the casing, giving accessibility for maintenance activities and easy access for the various seal gas supply and drain lines of the non driven end (NDE) shaft end seal. For very high pressure applications, shear rings will have to be used for the end cover. The casing contains an inner barrel with the stationary compressor diaphragms. Low-solidity vanes are installed in the diffuser in order to eliminate the occurrence of diffuser rotating stall and, secondly, to increase the compressor efficiency. In order to minimize diaphragm deflections due to the high-pressure loading, the inner barrel has integrated diaphragm support holders. The journal bearings are directly mounted into the casing and end cover, respectively. Also, the bearing support diameters in the latter components are used as a reference for further machining of the compressor casing. Aluminum labyrinths with small clearances are used in order to minimize seal leakage. Special attention is paid to keep the rotor concentric with the impeller and balance drum labyrinths. A minimum number of components are used in the path, from the bearing supports to the labyrinths, in order to reduce the buildup of tolerance fields.

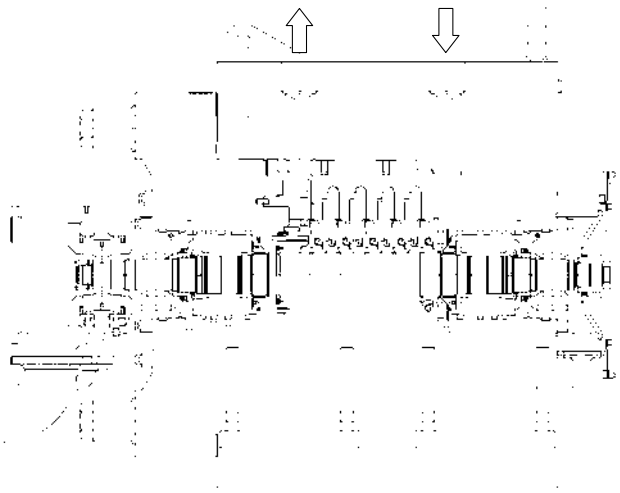

Figure 1. Cross-Sectional Drawing of the Reinjection Compressor.

In the case of a high-pressure compressor, it is highly advantageous for the user if it is possible to maintain small clearances in the labyrinth seals. Several disadvantages result from enlargement of the clearance in the labyrinth seals:

- The efficiency becomes poorer due to the increase in the flow circulating in the compressor.
- The load on the thrust bearing will change because of the change in the pressure distribution along both sides of the impeller as the leakage increases.
- The destabilizing forces from the labyrinths acting on the rotor become larger because the inlet swirl into the labyrinths becomes larger as the leakage increases.

The unwanted enlargement of the clearance in the labyrinth seals is often the result of inadequate centering or of high vibration amplitudes on passing through the resonance speed with a high amplification factor. High-pressure compressors have, as a natural design feature, relatively light and stiff rotors that usually exhibit high damping from the hydrodynamic bearings, i.e., the amplification factor is small and the resonance amplitudes are thus low. Good centering of the labyrinth seals can be ensured by means of various design measures. At a later point, this paper will deal with the calculation of the transient and stationary deformation of a special seal design on the balance drum. Measurements were executed in order to verify these calculations.

These examinations represent good examples of the design method described in this paper. All components that have an influence on the vibration behavior are examined both analytically and experimentally. The greater the attention paid to these examinations of the components, the greater the precision that can be applied when modeling the components within the overall system. The same also applies, of course, to the aerodynamic components (Wallmann, 2000). With this methodology, the designing can be performed with a high targeting accuracy. The disadvantages of superfluous measures are avoided and the required high degree of reliability with good efficiencies is ensured. Verification of the calculations by testing of machines at the test stand is utilized for validating the applied models.

Impellers

Radial impellers are subject to both static and dynamic loads. The predominant portion of the static load is generated by centrifugal forces.

A reliable method being used for a long time for calculating the deformations and stresses resulting from centrifugal force is the finite element analysis (FEA). In view of the cyclic symmetry of an impeller, it is adequate for this static calculation to model only a sector of the impeller. The validity of the analytical design is checked by means of an overspeed test according to API 617 (1995). Experience has shown that local stress peaks exceeding the yield stress do not basically represent a danger. The utilization of actual stress/strain curves in nonlinear FEA calculations shows that local redistribution of stresses occurs in such highly loaded impellers during an overspeed test. Within the operating speed range, however, the deformations remain fully within the elastic range.

The impellers are shrunk onto the shaft. The solid impeller hub and disk with the blades are manufactured from a single piece, while the shroud disk is brazed on or welded. This design serves to prevent stress peaks in the area of the impeller attachment and of the impeller disk. The design has proven itself, since there are no known cases in which this design has resulted in any damage due to static overloading.

A much more complex and demanding matter is the handling of dynamic impeller loads, which may lead to fatigue fractures. It is very difficult to ascertain the actual magnitude of the dynamic loads and a large degree of uncertainty is present here. A possible means of guaranteeing the operational reliability is to avoid excitation of impeller natural frequencies. The reason for this is that, as opposed to the absolute magnitude of the excitation, the frequency of the excitation can be predicted with great accuracy on the basis of known blade numbers and the machine operating speed range.

All the natural frequencies of an impeller can be determined if the entire structure is modeled instead of only a sector. The calculated modes of vibration can be ordered according to the number of nodal diameters and nodal circles (Rao, 1991). Above all in the case of speed-controlled machines, it cannot be avoided that the excitation originating from a vaned diffuser, for example, will coincide with one or more natural frequencies of an impeller. It is known from the work done by Campbell (1924) and from numerous more recent literature sources (Srinivasan, 1997; Wang, et al., 1999; Jansen and Fetfatsidis, 1999) that, as a function of the number of stationary and rotating blades, only those mode shapes can actually be excited that exhibit a “suitable” quantity of nodal diameters. For all other mode shapes, the coincidence between the excitation frequency and the respective natural frequency is considered to be safe.

Rotordynamics

The compressor has to be designed to run at low vibration levels over the entire operating speed range. It should not be sensitive to unbalance or other additional forces acting on the rotor.

With respect to the lateral rotor vibrations, a clear distinction must be made between forced vibrations and self-excited vibrations due to the fundamental differences involved.

Forced Vibrations

Forced vibrations are the less dangerous since their amplitude is relatively constant and, above all, limited. In centrifugal compressors for example, forced vibrations can arise due to unbalances at rotational frequency, shaft alignment errors at double rotational frequency, and diffuser rotating stall at around 10 to 20 percent of the rotational frequency. Proven remedies are low- and high-speed balancing, good alignment under consideration of possible thermal casing deformations, and the utilization of optimized diffusers. Low-solidity vaned diffusers make it possible largely or completely to avoid subsynchronous vibration components, with only minor reduction of the flow operating range. Low-solidity vaned diffusers have been successfully in operation for many years now.

Self-Excited Vibrations

When self-excited vibrations occur, they usually show up as subsynchronous vibration with a frequency close to the first critical speed. The API 617 Standard (1995) allows subsynchronous vibrations to appear during testing with an amplitude of not more than 20 percent of the permissible overall vibration level. In most cases, the root cause of self-excited vibrations is to be found in the bearings, in the fluid-film shaft seals, or in the labyrinth seals. As will be shown later, there is a certain margin between the onset of minor subsynchronous vibration and the stability threshold. Therefore minor subsynchronous vibrations are felt to be acceptable, if the design is based on a reliable rotordynamic analysis. However, the limits as stated in API 617 (1995) should not be exceeded too much in the field, since the amplitudes may rise quickly to excessive values upon crossing the stability threshold.

Evaluation of Rotordynamic Design

In order to assess the rotordynamic design of high-pressure compressors, the users often use the input of a number of parameters into a Fulton diagram (Fulton, 1984) or a Kirk-Donald diagram (Kirk and Donald, 1983) due to the simplicity of this procedure. In agreement with other manufacturers (Kirk, 1988; Memmott, 1999), the authors have the opinion that these diagrams are suitable only for an initial estimation of a design and that, since they disregard the design details, they do not allow any qualified statement to be made regarding stability. A decision regarding the amount of effort on the stability analysis, e.g., consideration of labyrinth seal forces, *can be based* on the result of such an initial assessment. The authors used an inhouse-developed diagram, shown in Figure 2, as a screening criterion. It uses, in addition to the Fulton diagram, the rotor mass as a further parameter. This considers the fact that a light rotor is more sensitive to aerodynamic excitation than a heavy rotor that has an identical flexibility ratio and that runs at the same gas density.

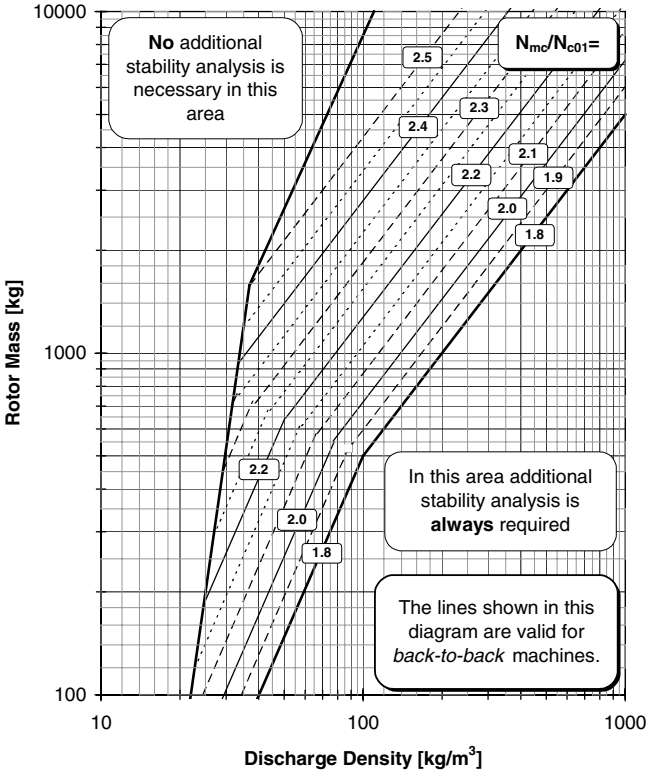

Figure 2. Screening Criterion Regarding Required Efforts for Stability Analysis.

All these diagrams confirm the findings made in the past (Kirk and Donald, 1983) that the robustness of a rotor system increases as the shaft stiffness increases. A proven robustness parameter is the flexibility ratio, which is defined as the ratio of the maximum continuous operating speed and the first critical speed for a rotor on rigid supports.

However, for a meaningful evaluation of a specific rotordynamic design, the details of the bearings and the seals have to be considered. These elements are discussed in the following paragraphs.

Bearings

The phenomena of oil-whirl and oil-whip in plain sleeve and fixed lobe bearings when a certain threshold speed is exceeded have been known for a long time. Therefore, in machines running above the first critical speed, tilting-pad journal bearings have become the most commonly used bearings since they do not have significant cross-coupled stiffness coefficients and thus do not show any limiting speed in practice. It has nevertheless been demonstrated by de Jongh and Morton (1996) that synchronous instability can occur even with tilting-pad journal bearings when incorporating the temperature gradient across the bearing journal into the modeling as an additional degree of freedom.

Figure 3 shows a typical journal cross section with a temperature profile established from four measured temperatures in the shaft journal. Due to the unavoidable residual unbalance, the orbit of the shaft in the journal bearing produces a temperature gradient locally across the journal cross-section and this can, under certain circumstances, lead to a continuous increase of shaft thermal bending and overhung unbalance. Up to now this type of self-excited vibration has been observed in machines with large overhung masses, relatively low bearing load, and high circumferential velocity. The machines, which may suffer from this mechanism, are drive-through machines and those machines equipped with particularly heavy couplings due to high power ratings. Problems of this type can be prevented by a rotordynamic analysis that takes into account the temperature gradients across bearing journals. It is necessary here to take into account the, to some extent, contradictory clearance requirements of the unbalance response calculation and the stability analysis. In critical cases, design measures have to be taken in order to lower the effect of the temperature gradient on the shaft bending. A possible solution, for which a patent has been applied, is the application of a heat barrier sleeve and has been described in de Jongh and van der Hoeven (1998). Kocur and de Jongh (2000) have presented two more case histories on this specific subject.

Fluid-Film Shaft Seals

In the past, floating ring type oil seals were very often used for the shaft sealing in high-pressure compressors. These seals introduce additional damping into the rotor bearing system, provided that the rotor operating speed is located below a value of twice the first critical speed. Vibration problems can occur when the radial movability of the outer seal ring is restricted (“lockup”) as a result of large axial forces acting on this ring. Good centering of this ring and additional damping can be achieved by integrating an additional tilting-pad bearing into this outer ring, as shown in Demag (1981) and Memmott (1992). The problems concerned with these floating ring shaft seals and the auxiliary oil supply system have resulted in the actual situation that only dry gas seals are being used in the great majority of cases for new machines. Care should be taken when machines supplied with floating ring shaft seals are to be retrofitted with dry gas seals. Several cases are known (Zeidan, et al., 1993; Kocur, et al., 1987) in which, due to the absence of the damping that had previously been provided by the floating ring shaft seals, the bearing damping was no longer adequate for stable running conditions. Negligent retrofitting with dry gas seals can therefore lead to instability in which the decisive factor is not the application of the new seals themselves but the lack of damping from the old seals.

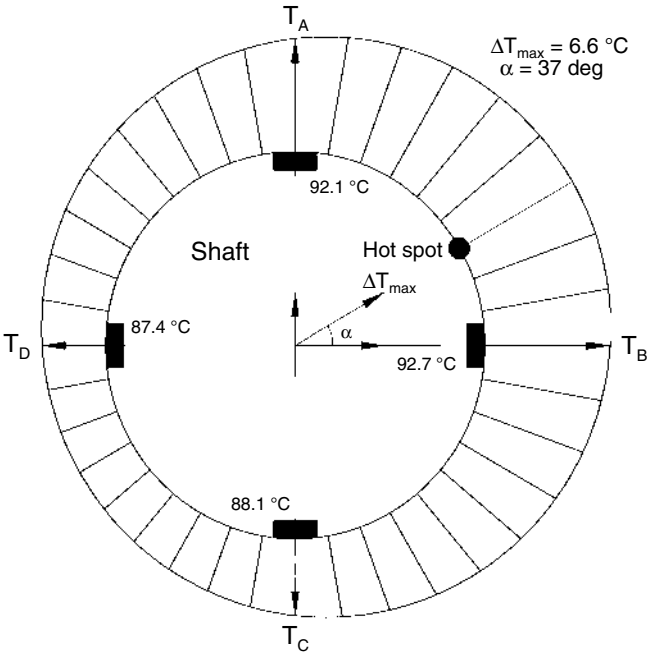

Figure 3. Cross-Section of Bearing Journal with Sinusoidal Temperature Distribution.

The various design types, the area of utilization, and the reliability of dry gas seals are described from the manufacturer’s point of view in Aarnink, et al. (1999). The variant most frequently used is the tandem dry gas seal, for which references are available today for sealing pressures up to 250 bar (3625 psi) and of which the boundaries of utilization are continually being extended. In the triple dry gas seals, which are used in only a few cases, the pressure drop is being reduced in two stages. Disadvantageous here is the added length to the rotor bearing span, and the increased effort in controlling the intermediate pressure and the crossflow.

Labyrinth Seals

The significance of labyrinth seals for the stability analysis becomes greater as the gas density increases. Along with the inlet gas density, the inlet swirl entering the seal is one of the main influencing variables. The initial comprehensive measurements of cross-coupled stiffness made by Benckert (1980) were related to relatively long seals used on balance drums. It rapidly became clear that, in addition to the destabilizing cross-coupled stiffness, damping forces would also necessarily be present and that the impeller eye seals would likewise need to be considered (Kirk, 1988).

In addition to these concurring opinions, the literature nevertheless contains a large number of contradictory statements.

Thus, according to Memmott (1999), consideration of the damping of impeller eye seals leads to unduly favorable stability results. In this paper, a negative direct stiffness of toothed labyrinths is being disregarded, since this could not be confirmed by measurement of the natural-frequency on compressor rotors. Childs (1993), on the other hand, reports that long labyrinth seals virtually always have a negative direct stiffness.

According to examinations by Millsaps and Martinez-Sanchez (1994), coupling to upstream conditions may have a strong influence on the dynamic coefficients of short labyrinth seals whereby the results may accordingly differ by up to a factor of four!

The objective of the examinations made by Baumann (1999) on two compressors was to check, by means of natural-frequency and damping measurements, the accuracy of the dynamic labyrinth coefficients that had been calculated using a finite-differences method. According to this report, the forces ensuing from the labyrinth seals influence not only the stability, but also the measured

natural frequencies. An unexpected drop in natural frequency tended to occur, depending on the labyrinth type used and the use of swirl brakes. It was not possible to explain all the observed phenomena, even though the calculated values were adapted to the measured values by reversing the sign for the calculated direct stiffness and by doubling all the other stiffness and damping coefficients. A fundamental problem of this procedure may be that on the machine itself the rotordynamic influences of all seals and of both journal bearings become superimposed on one another and this makes a clear allocation of the various influences difficult to achieve.

Deswirling at Seal Entrance

The strong influence of the gas inlet swirl, upstream of the labyrinth, on the magnitude of the cross- coupled stiffness was first verified by Benckert (1980) and has been confirmed by various other investigators. The book of Childs (1993) provides a good survey. A result of this knowledge is that several design measures have been developed for reducing the inlet swirl: shunt-holes (Memmott, 1992), jet injection in opposite direction to shaft rotation (Brown and Hart, 1986; Kirk, 1988), and swirl brakes in two different designs (Wyssmann, et al., 1987; Wagner and Steff, 1996).

Shunt-holes have proven their positive influence in many machines that show stable operation, even though some cases are known in which they have not produced a satisfactory effect (Gelin, et al., 1996; Kuzdzal, et al., 1994; Sorokes, et al., 1994). The disadvantage when using shunt-holes is the resulting enlargement of the bearing span (Figure 4). The requirement that the rotor should have the largest possible stiffness (for which the shortest possible bearing span should be implemented) runs contrary to the idea of employing shunt-holes also on impeller eye seals and not just on the balance drum labyrinth. A further disadvantage is the loss of efficiency caused by shunt-holes. A doubling of the leakage was ascertained during the investigations made by Azuaje (1997) on labyrinths with shunt-holes installed. It may therefore be useful to look for other effective measures for inlet swirl reduction that do not exhibit the disadvantages mentioned above.

A design version of shunt-holes comprises jet injection in opposite direction to shaft rotation. This version, however, still does not avoid the above disadvantages. Jet injection in opposite direction to shaft rotation enables the sign for the cross-coupled stiffness to be reversed, which in the purely formal sense does bring about a very high effective damping ($C_{eff} = C(1 - k/C\omega)$). The consideration of effective damping for the forward mode only involves the danger of neglecting the destabilization of the backward mode. This stability problem has already been pointed out by Brown and Hart (1986).

An alternative solution is to be found in the use of swirl brakes. These can be arranged at the outer edge of the impeller sideroom or directly in front of the labyrinth seal. The use of swirl brakes at the outer edge of the impeller sideroom has the advantage of reducing the axial thrust. The disadvantage of this design, however, is the loss of efficiency as a result of the rise in pressure in the impeller sideroom. According to Baumann (1999), this can amount up to more than 8 percent.

In the interests, therefore, of the highest possible degree of efficiency and of a short and thus stiff rotor, the arrangement of swirl brakes directly in front of the labyrinth seal appears to be the best possibility for reducing the inlet swirl (Figure 5).

A number of authors (Wyssmann, et al., 1987; Bromham, et al., 1996) have made the assumption that swirl brakes serve to virtually eliminate the cross-coupled stiffness and to maintain the damping in its full magnitude. This would then cause the logarithmic decrement to become enlarged as the gas density increases. However, the papers of Wagner and Steff (1996) and of Wagner (1999), which are dealt with in greater detail below, show that this assumption is not correct. Their experimental findings are supported by recent numerical investigations of Nielsen, et al. (1999), and Nielsen, et al. (2000).

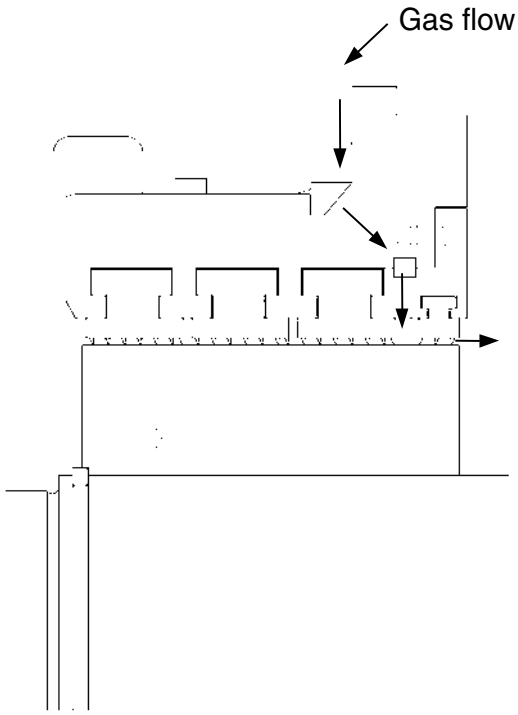

Figure 4. Inlet Swirl Reduction by Shunt-Holes.

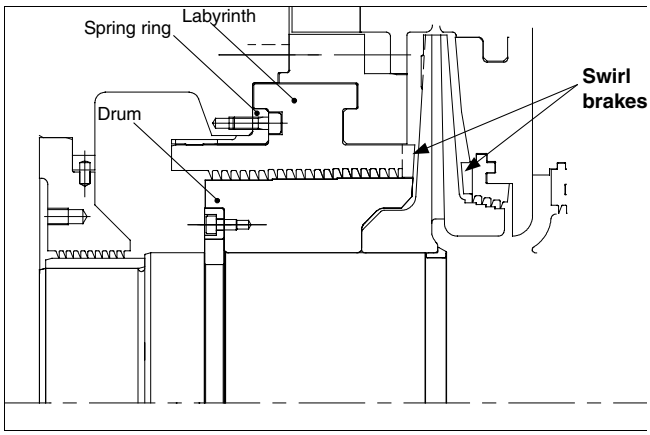

Figure 5. Inlet Swirl Reduction by Swirl Brakes.

Honeycomb Seals

There are several technical papers that indicate that the replacement of the balance drum labyrinth seals by honeycomb seals has been able to solve stability problems in compressors (Gelin, et al., 1996; Zeidan, et al., 1993; Sorokes, et al., 1994). Problems are caused, however, by the need to obtain a picture of the dynamic behavior of honeycomb seals in the rotordynamic models that is compatible with real conditions. This makes it difficult to perform a reliable anticipatory calculation of the limits of application. “Erratic and puzzling results” are mentioned in the summary indicated by Childs (1993) of the results of examinations at Texas A&M University. Small changes in the geometry of the honeycombs measured led to large deviations in the dynamic coefficients. According to the analytical findings contributed by Kleynhans and Childs (1996), honeycomb seals cannot be described by the spring/damper model that is valid for labyrinths, but require a more general manner of describing their dynamic characteristics in the frequency domain. This view is supported by the measurements made by Wagner (1999). For this reason, the

measured rotordynamic behavior of a machine equipped with honeycomb seals may deviate strongly from the calculation if these honeycomb seals have been modeled by spring/damper coefficients only.

Labyrinth Test Rig

It is clear from the explanations given above that there has been a considerable knowledge improvement during the past 20 years relating to the influence of labyrinth seals on the onset of self- excited vibrations. Nevertheless, today there are still a large number of contradictions and gaps in this knowledge that hinder the execution of a reliable rotordynamic stability analysis.

A brief description is given below of the procedures followed for solving the above-mentioned problems within the company that employs the two leading authors.

First, it has been decided that the global concepts for the evaluation of rotor stability were inadequate for analyzing and optimizing the design details and that there was an urgent need to ascertain the spring and damping coefficients of individual seals. Identification of individual spring and damping coefficients on a complete compressor unit did not seem to be very promising, because, in a centrifugal compressor, the influences of all seals and bearings become superimposed on the rotor vibration behavior. Besides that, it is very difficult to establish accurately the threshold conditions of a machine. Therefore it was decided to design a component test rig that would enable the actual labyrinth seal conditions to be simulated in all respects and minimize any kind of extrapolation. This high-pressure test rig is described in more detail in Wagner and Steff (1996). In this rig, the shaft is supported by magnetic bearings that are used at the same time to establish the labyrinth forces acting on the rotor. Figure 6 shows a cross- sectional drawing of this test rig. The highest priority was given to precision in the manufacturing of test seals as well as in the entire measuring technology in order to obtain reliable data. The design of the test rig makes it possible to vary all the important parameters such as upstream pressure, back pressure, rotor speed, inlet swirl, and all the geometrical parameters independently of one another, and thus to measure their influence on the dynamic labyrinth coefficients. The testing method employed does not only provide the cross-coupled stiffness and direct damping, but also the direct stiffness and the cross-coupled damping. The two latter should not be neglected for high-pressure compressors, since they may lead to a significant change in the rotor's natural frequency, which in turn is decisive for the rotor's sensitivity. Up to now, the range of tests that has successfully been executed covers more than 30 different seal configurations and also includes honeycomb and brush seals. The total number of individual test points comes to more than 1700. A comprehensive and systematically generated database is thus made available, which is being used for reliable rotor stability analyses. These measured data can furthermore be used for the calibration of analytical models for calculating the dynamic labyrinth coefficients.

SPECIFIC COMPRESSOR DESIGN

The following part of this paper describes a specific high-pressure reinjection compressor. This natural gas reinjection compressor unit has been applied on a floating production, storage, and offloading vessel (FPSO) in the North Sea, located 280 km (150 miles) east of Aberdeen. The compressor is directly driven by a 5500 kW (7473 hp) gas turbine at a rated speed of 11,896 rpm (100 percent). The operating speed range was defined as 9517 rpm to 12,491 rpm (maximum continuous speed). The design flow is around 600 m^3/hr at suction conditions of 172 bars (2494 psi) at 30°C (86°F), and the maximum discharge pressure is 418 bars (6061 psi). Table 1 shows some general information on this compressor unit.

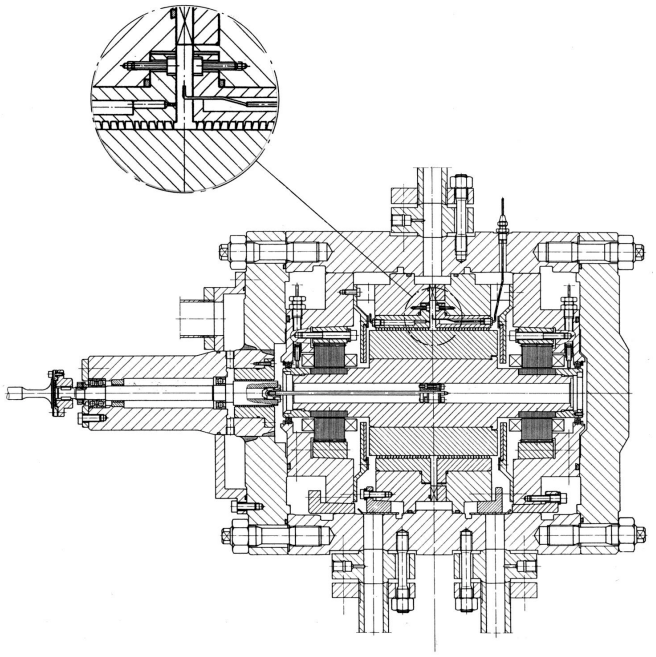

Figure 6. Cross-Sectional Drawing of the Labyrinth Test Rig.

Table 1. General Compressor Design Rates.

Description	Units		
Rotor speed (100%)	rpm	11,896	
Suction pressure	Bara (Psia)	171.5	(2487)
Suction temperature	DegC (DegF)	30	(86)
Discharge pressure	Bara (Psia)	418	(6061)
Discharge temperature	DegC (DegF)	103	(217)
Shaft power	KW (HP)	5,500	(7473)
Gas density (discharge)	kg/m3	263	
First critical speed Nc1	rpm	7,100	
Flexibility ratio	-	1.78	
Second critical speed Nc2	rpm	22,500	

In Figure 1, a cross section of the machine is given. The total rotor mass is around 300 kg (660 lb), and the rotor is supported by two fluid-film, tilting-pad type journal bearings and one double acting tilting-pad type axial bearing. Two triple dry gas seals are used in order to seal the machine at both shaft ends. The pressure drop of these seals is being taken by the two inner seal rings, whereas the third (outer) seal ring is subjected to a small differential pressure only.

Impellers

For this compressor application, small flow coefficient 2D impellers were applied. At maximum continuous speed, the impellers have a tip speed of 232 m/s (761 ft/sec). The stress thus arising at the most highly loaded zone in the impeller is less than 350 N/mm^2 (50,750 psi). This impeller is therefore subject to very low static loads.

Because of the high gas density in combination with low-solidity vanes, significant dynamic excitation forces on the impellers were expected. A finite element study was executed to establish the location of impeller natural frequencies in order to prevent resonance conditions. Also, an experimental modal analysis test was executed to confirm the calculated impeller natural frequencies.

Figure 7 shows various mode shapes of vibration including the umbrella mode and the mode shapes of the first eight nodal diameters from the FEA study. For the condition of resonance vibrations, it is not sufficient to simply have coincidence between an excitation frequency and an impeller natural frequency. It is also

necessary for the profile exhibited over the circumference by the exciting pressure distribution to conform to the deflections of the mode shape. The resonance diagram shown in Figure 8 is suitable for checking whether the excitation arising from a vaned diffuser will cause an impeller to become resonant. In the present case, the number of vanes of the impeller (z = 17) and of the diffuser (z = 10) were selected such that only the mode shape with seven nodal diameters could be excited by the pressure profile of the vaned diffuser. The second harmonic of this pressure profile would be able to excite the mode shape with three nodal diameters, and the third harmonic would excite the mode shape with four nodal diameters. Since, however, these harmonics have much smaller amplitudes than the basic profile, they are normally not taken into consideration.

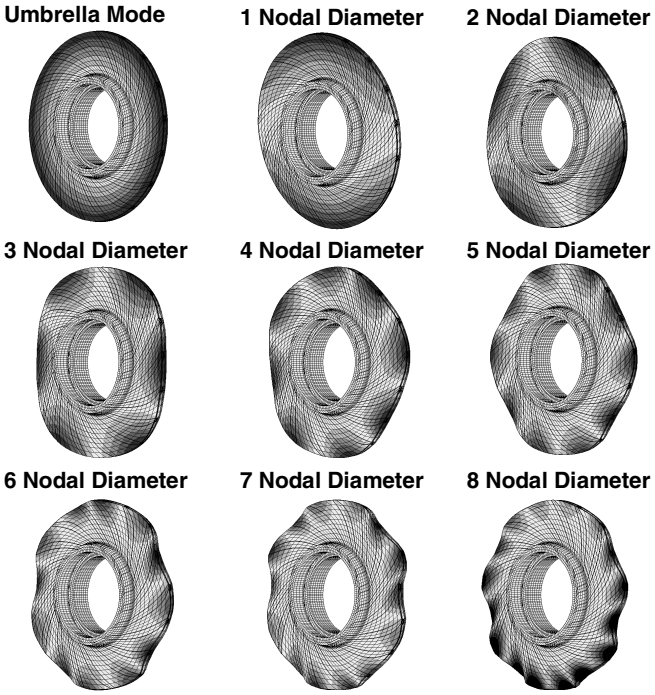

Figure 7. Predicted Mode Shapes of a Centrifugal Impeller.

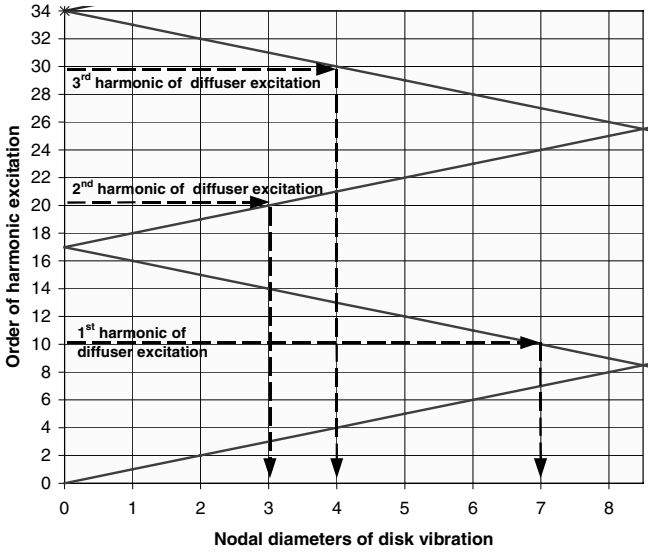

Figure 8. Resonance Diagram in General Form.

The representation of the measured results of one of the impellers in Figure 9 is somewhat complex by the need to check the entire speed range from 70 percent to 105 percent of the design speed. It can nevertheless be recognized that the natural frequency that belongs to the mode shape with seven nodal diameters is located much higher than the excitation frequency. The above-mentioned excitations originating from the second and third harmonics of the pressure profile are located above the natural frequencies with three and four nodal diameters. The coincidence that can be seen in Figure 9 between the second natural frequency and the excitation that arises at minimum speed does not represent any danger because the pressure profile is not able to excite this mode shape with two nodal diameters. There are therefore no resonance conditions present and, accordingly, it can be concluded that the design of the impellers is sound.

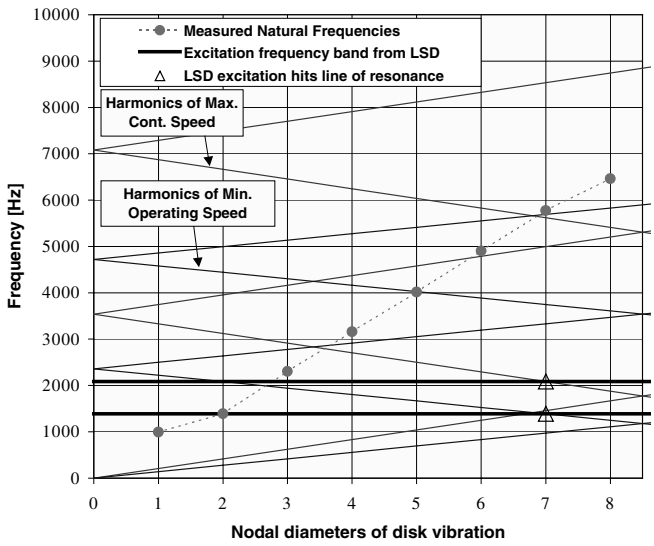

Figure 9. Measured Natural Frequencies of the Fifth Stage Impeller.

Balance Drum Labyrinth Seal

Control of the labyrinth seal clearances is especially essential for the balance drum labyrinth because of the high differential pressure. In order to minimize the leakage, the labyrinth clearance should be kept as small as possible. However, there should not be any risk of a rotor rub during startup or at any other significant running condition. A time-transient finite element analysis was executed in order to simulate the labyrinth clearance during a cold startup. Besides the variations of gas pressure and temperature during such a startup, the rotordynamic behavior, including the passing of the first critical speed at around 7100 rpm, was taken into account. Figure 5 shows a cross section of the balance drum and the labyrinth behind the last stage impeller, whereas an axisymmetric finite element model of these two components is given in Figure 10. The balance drum is made of steel and the labyrinth is made from aluminum. During startup, the rotating drum will grow due to the centrifugal force and the thermal loading. The stationary labyrinth will deform due to the influences of the gas pressure and the temperature. The time transient load steps for the rotor speed, the gas pressure, and the temperature are given in Figure 11. Worst case operating conditions were used for this analysis, being a compressor startup within 10 seconds against the surge control line. In Figure 12, the results of the transient startup analysis are given in terms of balance drum (dashed lines) and labyrinth (solid lines) growth rate up to 600 seconds from the start. Figure 13 gives the calculated clearance between the balance drum and the labyrinth for the same analysis. As can be seen, at the middle and high-pressure side of the labyrinth, the clearance

reaches a minimum value after around 30 seconds. The low-pressure side clearance increases continuously from the start. Figure 14 shows the deformations of the FEA model superimposed for several time instants.

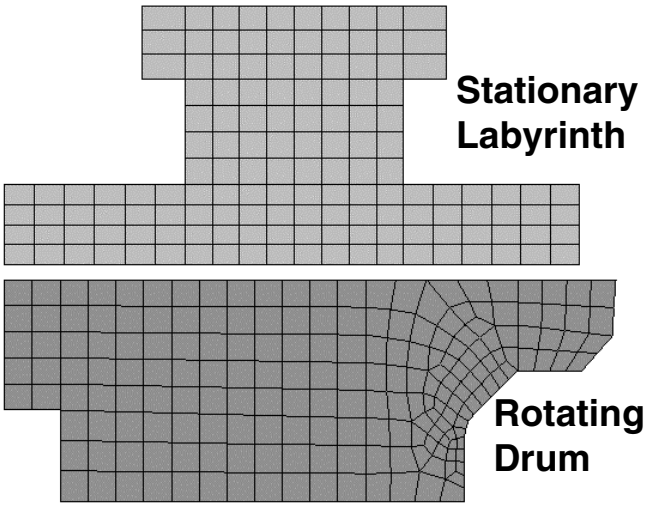

Figure 10. Finite Element Model of Balance Drum Seal.

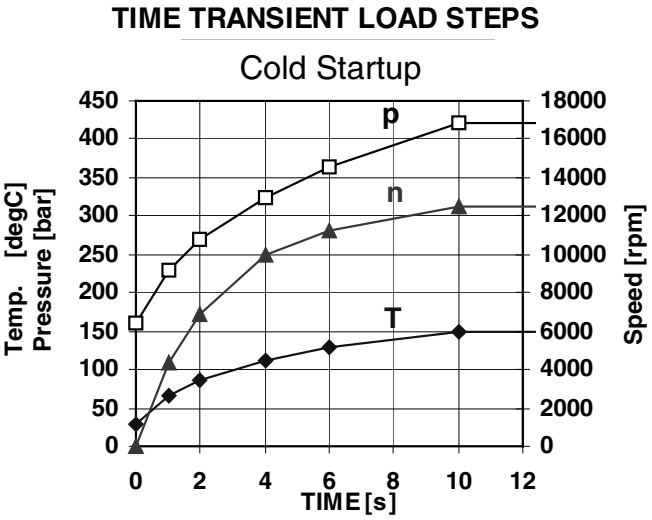

Figure 11. Load Steps for Time Transient Analysis.

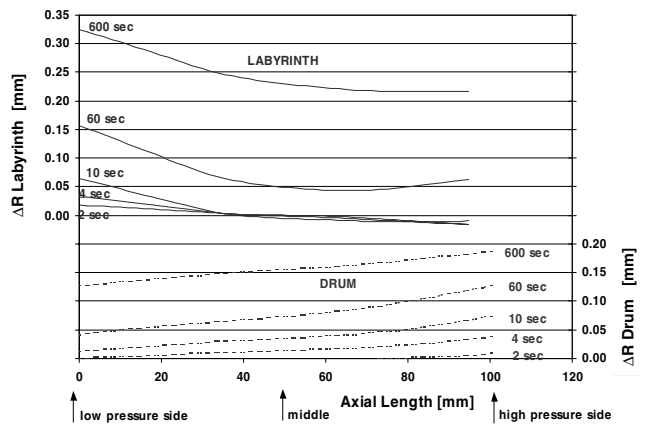

Figure 12. Result of Time Transient Analysis.

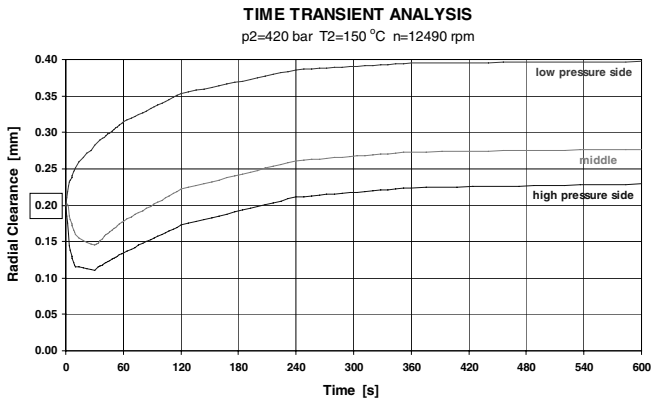

Figure 13. Predicted Clearance from Time Transient Analysis.

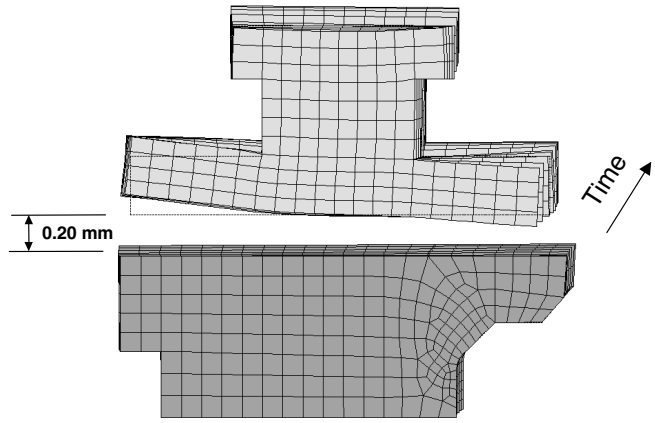

Figure 14. FEA of Balance Drum Seal, Deformations Superimposed for Several Time Instants.

The analysis results showed that the operating stresses stayed within acceptable levels. However, due to the difference in thermal growth between aluminum and steel, the labyrinth loses contact with the radial support structure. A special spring ring has been designed to keep the labyrinth in its position, concentric with the rotor. During testing at the test stand, the relative position of this labyrinth to the rotor balance drum has been experimentally verified.

As an additional detailed study, the labyrinth teeth geometry has been analyzed for deformation and stress at steady state conditions. Figure 15 gives the deformed labyrinth teeth due to a differential pressure of 20 bars (290 psi) and a pressure of 420 bars (6090 psi) at the high-pressure side. The maximum equivalent stress for this loading amounts to the low value of around 54 N/mm^2 (7830 psi) and the maximum deformation at the tip location was only around 0.01 mm (0.5 mil).

Rotordynamics

Nowadays it is common practice to pay specific attention to the rotordynamic design of high-pressure compressors. This is strongly supported by the screening criteria as mentioned above.

Some fundamental criteria related to the required separation margins of critical speeds and to the vibration amplitudes in relation to running clearances are provided by API 617 (1995). For the subjected rotor design, fulfillment of the API criteria was not very difficult. The first critical speed on hydrodynamic bearings is the highly damped first bending mode (AF = 2.55) at around 7100 rpm. The minimum operating speed is at 9517 rpm, thus the separation margin is more than 25 percent. The second bending mode is located at around 22,500 rpm, which is far above the maximum operating speed.

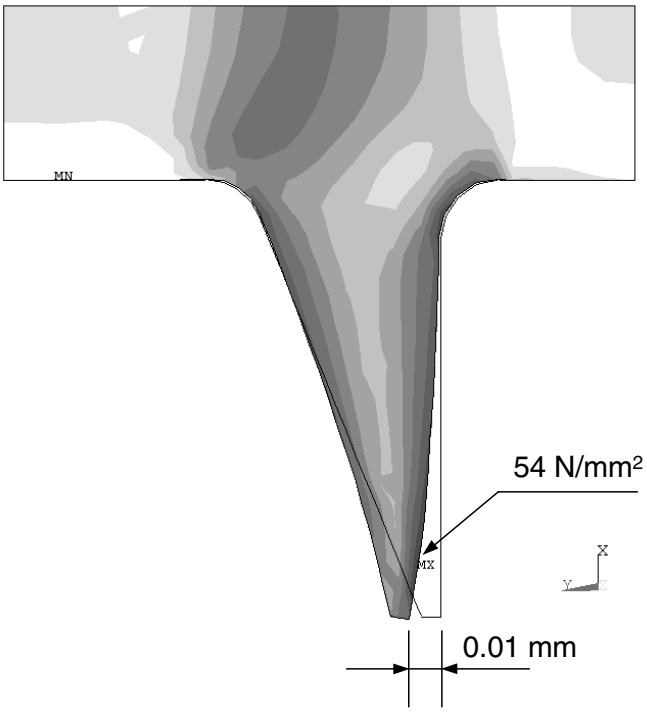

Figure 15. Labyrinth Teeth Deformation Predicted with FEA.

The investigation of thermal rotor instability, as mentioned before, showed also that no problems are to be expected. The real part of the gain vector, which is decisive for thermal stability, exceeds the stability limit at speeds above 14,300 rpm, which is far enough above the maximum continuous operating speed.

Thus the most important investigations are related to rotor stability. At this instant, it should be mentioned that some difficulties came up due to the very short delivery time that was agreed upon. In order to meet the customer's shipping date, the design phase commenced during the negotiations. The original design was based on a tandem dry gas seal, but it turned out that the customer preferred a triple dry gas seal. This demand led to an increase in bearing span and a degradation of rotor stability. The flexibility ratio increased from 1.63 to 1.78, and the predicted logarithmic decrement for the worst case condition dropped from a value of $\delta = 0.13$ to a value of $\delta = -0.24$, indicating an unstable rotor. However, the original design did not utilize swirl brakes in front of the labyrinth seals. This potential had to be used for the revised design with the increased bearing span.

In Figure 16, the decrease of the logarithmic decrement with increasing gas density is shown for different predictions. The dashed lines represent the situation without swirl brakes for minimum and maximum bearing clearance. It is evident that the compressor would become unstable at about 80 percent of the design density, if the tight bearing clearance applies. In contrast to this, stability can be expected for all bearing clearances if swirl brakes are used, as shown by the solid lines.

Although the result as given in Figure 16 is most important, it is also worth looking somewhat deeper into this subject. Apart from evaluating only the logarithmic decrement, it is felt to be necessary to analyze the natural frequencies and how the seal forces affect them as well. A powerful tool for such an analysis is the generation of a root locus map, which shows the logarithmic decrement (real part of the eigenvalue, plotted as ordinate) and the corresponding natural frequency (imaginary part of the eigenvalue, plotted as abscissa) together. The "roots" (= eigenvalues = logarithmic decrement + j* frequency) as predicted from the eigenvalue analysis will change their location in this diagram when destabilizing forces are acting on the rotor system. The resulting

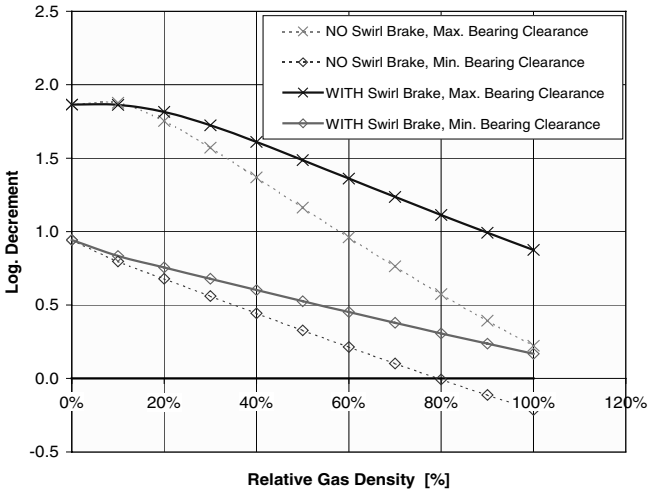

Figure 16. Logarithmic Decrement Versus Gas Density.

curves can be parameterized, e.g., with gas density. When this curve changes due to an increasing gas density from the half-plane of positive logarithmic decrement into the area of negative logarithmic decrements (i.e., a change of sign of the logarithmic decrement from a positive number to a negative number), instability occurs. Then it can be seen directly from the intersection of this curve with the frequency axis what the frequency of the subsynchronous vibration would be. Such a root locus curve is shown in Figure 17 for the situation with minimum and maximum bearing clearance, both with and without swirl brakes. In accordance with Figure 16, it can be detected that instability occurs for minimum bearing clearance if no swirl brakes were applied (dashed line). From Figure 17 it can now be detected that the frequency of subsynchronous vibrations will occur at somewhat higher frequencies for the compressor at full pressure compared with the unloaded machine. It was also found in contrast to other investigations (Baumann, 1999) that the labyrinth design used here has only a small impact on the frequency of the eigenvalue. However, the seal forces have a much stronger effect on the frequency of the highly damped eigenvalues, but they will not show up in practice due to their still very high damping.

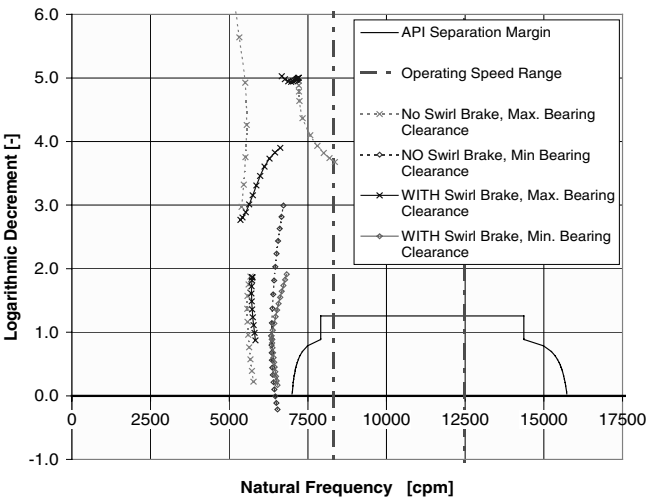

Figure 17. Root Locus Curve for Variation of Gas Density from Zero to 100 Percent.

The predictions for a staggered labyrinth seal, which were performed for comparison, show a drop in the natural frequency for the eigenvalue with low damping, which is due to the relatively high negative direct stiffness and the cross-coupled damping of the

staggered seal. However, due to practical design considerations, a straight-through labyrinth is used here for the balance drum.

After extensive investigation of different scenarios, it was concluded that the compressor design would be safe and reliable with the increased bearing span if labyrinth inlet swirl brakes are applied. Since the design showed that without the swirl brakes the rotor would become unstable, this gave us the possibility to verify the rotordynamic analysis and the applied dynamic labyrinth coefficients. Therefore it was decided to execute an additional PTC-10 (1997) Class I test without the swirl brakes installed in order to verify the predicted rotor stability threshold.

EXPERIENCE FROM COMPRESSOR TESTING AND OPERATION

General Test Setup

Successful testing of high-pressure compressors as described in Demag (1981) and ASME PTC-10 (1997) Class I testing with natural gas (de Jongh, et al., 1989) requires extensive experience.

Figure 18 shows the compressor on the test stand. The compressor has been tested simultaneously for thermodynamic and mechanical performance in the same test setup. Figure 19 shows a scheme of the test setup with the closed loop system. For reference and general comparison purposes, an ASME PTC-10 (1997) Class III test with test gas nitrogen was run first (Aarnink, et al., 1993). Directly after that test, an ASME PTC-10 (1997) Class I test was run in the same test setup and witnessed by the customer. Prior to this high-pressure test with natural gas, a safety full pressure test was run with nitrogen. During the tests, the compressor was driven by a variable speed electric motor via two shop gearboxes.

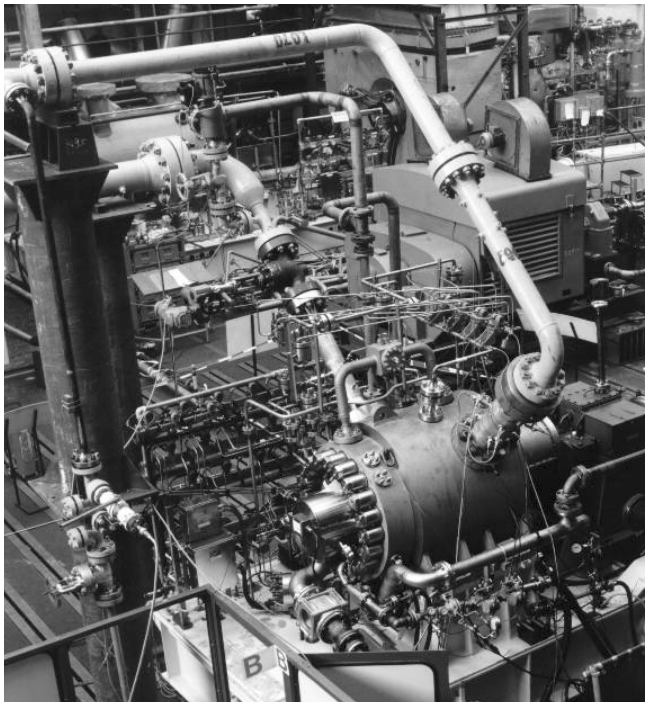

Figure 18. Reinjection Compressor on the Test Stand.

For the Class I test, liquefied natural gas (LNG) was used. This LNG was delivered in several trucks, and, during testing, gas had to be supplied continuously to keep the loop at the required pressure, taking into account the leakage from the loop due to sealing and cooling purposes of the triple dry gas seals (refer to Table 2 for the composition of the natural gas). In order to obtain the correct compressor volume ratio, molecular weight, and gas density, 12 percent carbon dioxide (CO_2) had to be supplied to the loop by an individual small booster compressor. The density of the gas in the loop was monitored continuously during testing and both LNG and CO_2 had to be supplied. Gas samples were taken at each measuring point for later analysis and for thermodynamic performance calculations. During the thermodynamic performance test with natural gas, the API 617 (1995) mechanical running test was executed.

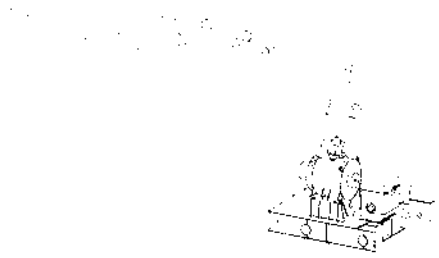

Figure 19. Scheme of Closed Loop Test Setup.

Table 2. Gas Composition LNG.

Gas Component	Formula	Fraction X (mol)
Helium	He	.00009
Nitrogen	N2	.01408
Methane	CH4	.91797
Ethane	C2H6	.05279
Propane	C3H8	.01171
n-Butane	C4H10	.00252
n-Pentane	C5H12	.00057
n-Hexane	C6H14	.00027
Carbon dioxide	CO2	.00000
Total		1.00000

Balance Drum Labyrinth Testing

During testing, the balance drum labyrinth clearance had been experimentally verified. Four displacement sensors were mounted into the labyrinth, spaced 90 degrees, at the low-pressure side (Figure 20). Prior to installation, these sensors were calibrated and functionally checked in a high-pressure bottle at pressures up to 200 bars (2900 psi). The balance drum had also been extended at the low-pressure side with an additional ring for the sensors to observe. A high-pressure feed-through was used to transfer the electrical sensor signals through the casing wall. Several temperature sensors were mounted as well in the aluminum labyrinth for temperature verification purposes.

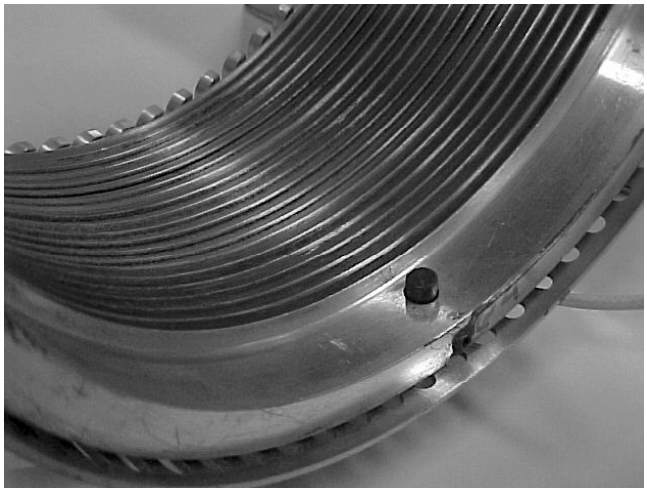

Figure 20. Displacement Sensors in the Balance Drum Labyrinth Seal.

Since the cold startup at the test stand was slower than the worst case condition, as considered in the time transient analysis, new time transient load steps were established from the actual startup at the test stand. With these boundary conditions, a new FEA study was prepared. Figure 21 shows the results from this analysis, including the measurement results. It can be seen that good correlation was obtained between calculation and test. Based on this verification result, it was assumed that the FEA calculation of the faster startup, mentioned before, is reliable. These experiments also confirmed that the designed spring ring, for the centering of the aluminum labyrinth, was functioning properly.

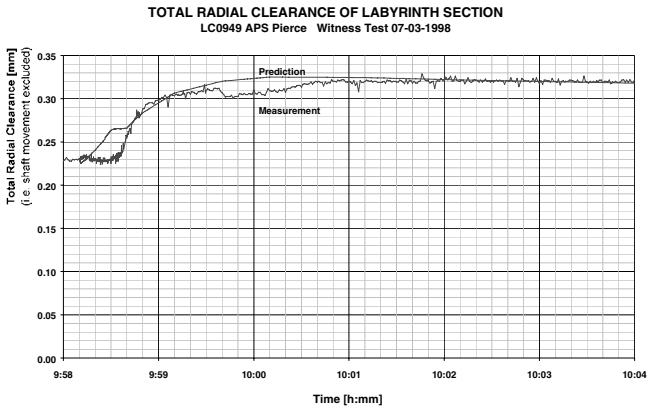

Figure 21. Calculated and Measured Labyrinth Clearance During Startup.

Mechanical Testing

In order to take into account the mechanical aspects, the thermodynamic performance test with natural gas was also executed in accordance with the API 617 Standard (1995). Since rotor stability is one of the main issues for high-pressure compressors, additional testing was executed to verify the margin to the onset of instability. It was calculated that the rotor would become unstable when the integral swirl brakes of the balance drum and the impeller eye labyrinths were not in place. So, additional labyrinths without swirl brakes were manufactured and tested in the compressor in order to confirm the calculations.

The first test series were conducted *with swirl brakes* installed. The complete ASME PTC-10 (1997) Class I testing was accomplished without any occurrence of subsynchronous vibration. A typical waterfall plot of these test runs *with swirl brakes* is shown in Figure 22. So far, it has been confirmed that, in agreement with the analysis, the compressor runs stable and safe.

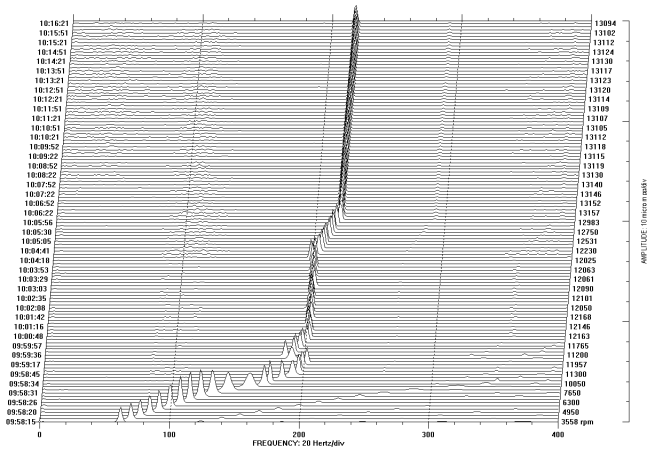

Figure 22. Waterfall Plot of Test Run with Swirl Brakes Installed.

For the second test series, the impeller eye seals and the balance drum labyrinth were replaced by seals *without swirl brakes*. For this specific test arrangement, it was expected to reach the onset of instability.

The first stability test was conducted at 80 percent speed and a lube oil supply temperature of 42°C (108°F). The discharge pressure was increased in steps of approximately 30 bar (435 psi), commencing at 160 bar (2320 psi), with continuous and careful observation of the spectra displayed on a frequency analyzer. At a discharge pressure of 360 bar (5220 psi), subsynchronous vibration came up to a level of about 10 µm peak-to-peak (0.4 mil peak-to-peak). This level of subsynchronous vibration was taken as "just stable, but close to instability." The result of the rotordynamic analysis for this operating condition is given in Figure 23. According to this diagram, the logarithmic decrement was around a value of $\delta = +0.10$ at 360 bar (5220 psi), 80 percent speed. The instability was predicted to occur at around 390 bar (5655 psi). For the sake of comparison, the solid line representing the as-designed condition with swirl brakes is also shown. The logarithmic decrement for this operating condition *with swirl brakes* would be above a value of $\delta = 0.50$, a comfortable safety margin.

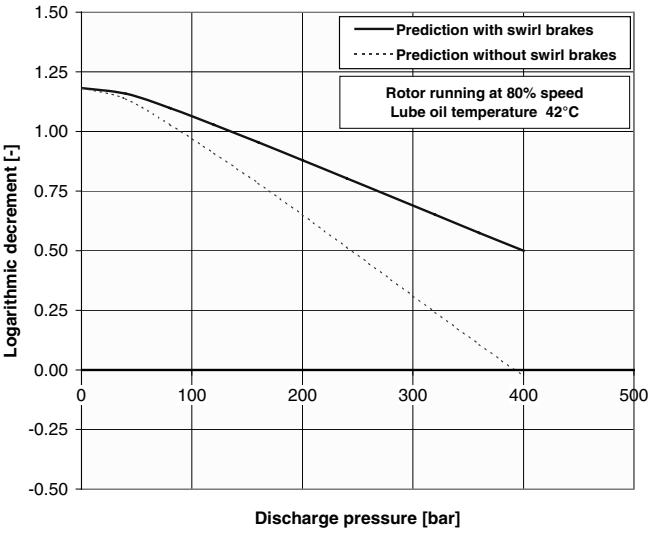

Figure 23. Rotordynamic Analysis of First Test Run.

After this first test, the rotor speed was increased quite rapidly in order to repeat this test at 90 percent speed. However, the pressure rise experienced during this acceleration was so high that the stability threshold was exceeded and the unit tripped on high vibration. From Figure 24 it can be found that the synchronous component was fairly constant, but a subsynchronous component came up at 105 Hz and within a few seconds the amplitudes were so high that a machine trip was initiated. The sudden increase of the *frequency* of the subsynchronous component in Figure 24 can be explained with a mechanical rub in the seals, which reduces the effective bearing span and thus increases the stiffness, resulting in an upward shift of the natural frequency. It was decided to start up the compressor again for continuation of the tests and the inspection conducted after finalization of this testing revealed some damage to the test seals without swirl brakes. The labyrinth clearances after this rub were about 50 percent above the values of the new parts. Thus, the increased clearance and its adverse effect on the rotor stability needs to be considered in the comparison theory/experiment of the further tests.

Continuation of testing was related to the approach of the stability threshold at higher speeds. At 90 percent, 100 percent, and at 105 percent of rated speed, the discharge pressure was increased again until the onset of subsynchronous vibration of about 10 µm peak-to-peak (0.4 mil peak-to-peak) was observed. Since the subsynchronous vibration shows up in the frequency spectrum with

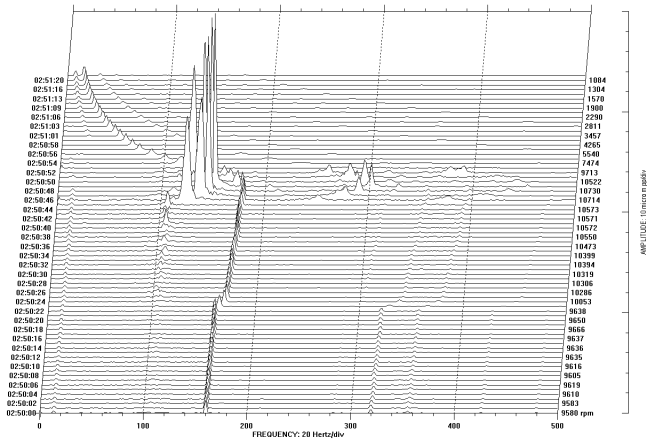

Figure 24. Waterfall Plot of Trip During Acceleration (without Swirl Brakes).

some fluctuations, it is difficult to define precisely the operating condition for the onset of subsynchronous vibration. In Figure 25, the two trips experienced during this testing are shown. The solid line in this diagram provides the predicted stability threshold ($\delta = 0$) and the dashed and the dotted line reflect the conditions for which a logarithmic decrement of $\delta = +0.2$ and $\delta = -0.2$ are predicted, respectively. The two trips are very close to the predicted stability threshold ($\delta = 0$), with some deviation to the safe side. With this figure, the onset of subsynchronous vibration can be related approximately to a logarithmic decrement of about $\delta = +0.05$ to $\delta = +0.10$. From the result taken at 100 percent speed, we can draw the conclusion that there is a difference of about 35 bar (500 psi), which complies with about 8 percent of the design pressure, from the onset of subsynchronous vibration in the order of 10 µm peak-to-peak (0.4 mil peak-to-peak) to the trip. Of course, these numbers may change for different compressors. Nevertheless, they may give some guidance in the assessment of subsynchronous vibration.

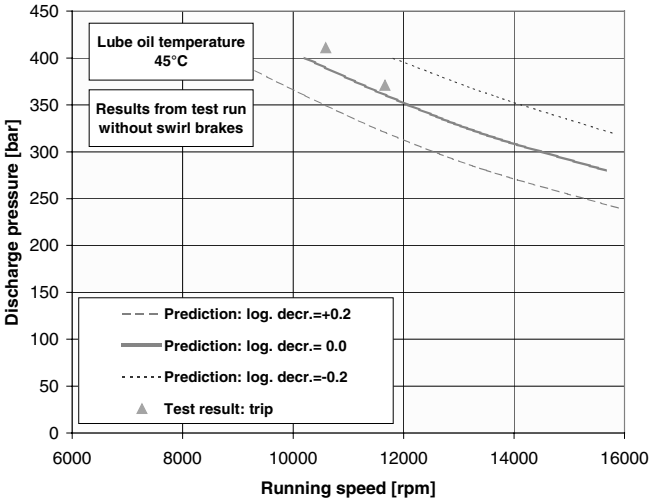

Figure 25. Predicted and Measured Stability Threshold.

Another test was performed regarding a variation of the lube oil supply temperature, since the analysis did show some sensitivity to this parameter as well. For this test, the compressor was run constantly at its maximum continuous operating speed at a discharge pressure of 200 bar (2900 psi). Starting with a supply temperature of 45°C (113°F), no subsynchronous vibration was present. Upon exceeding a supply temperature of 60°C (140°F), which is 10°C (18°F) above the rated temperature, some small amplitudes below 4 µm (0.16 mil) at 107 Hz came up, as shown in Figure 26. The prediction for this situation with worn seals gave, according to Figure 27, a logarithmic decrement of about $\delta = +0.15$ for this operating condition. As shown in Figure 28, this small subsynchronous vibration vanished completely after a minor reduction in speed.

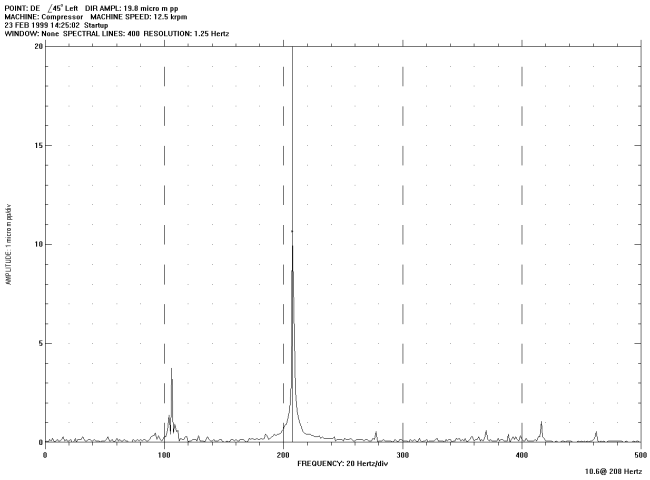

Figure 26. Vibration Spectrum at Elevated Lube Oil Supply Temperature.

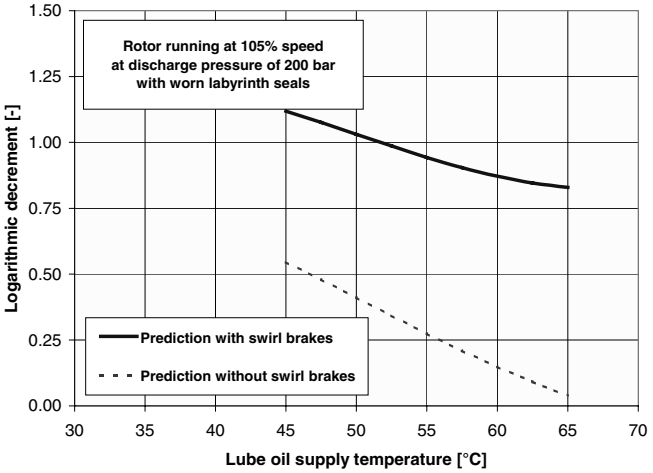

Figure 27. Predicted Effect of Lube Oil Supply Temperature on Rotor Stability.

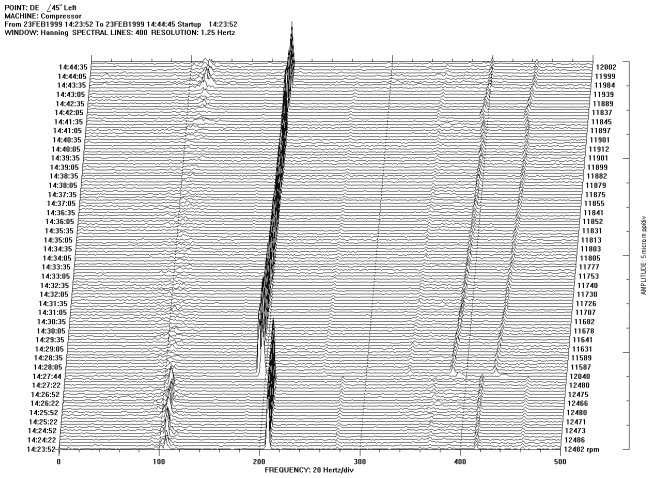

Figure 28. Waterfall Plot Taken at Elevated Lube Oil Supply Temperature.

These tests validated the applied rotordynamic model and the considerations applied for the bearings and the labyrinth seals, since the measured stability threshold itself as well as the frequency of the subsynchronous vibration were in good agreement with the predictions.

When approaching surge, a small component of diffuser rotating stall was detected. At a discharge pressure level of 420 bars (6090 psi), 6 µm peak-to-peak (0.24 mils peak-to-peak) was measured. Because of the frequency (around 10 to 20 percent of rotational frequency) and the linear relation to gas density, these vibrations were defined as diffuser rotating stall. Since the vibrations are of the forced type and the vibration levels are very low, they were established as harmless. Further investigation is being carried out in order to explain that rotating stall was possibly present upstream of the low solidity vanes. Additional experiments are being carried out in single-stage test facilities (Buse, et al., 1996).

Field Experience

After extensive testing at the manufacturer's test stand, the compressor unit was shipped to the FPSO in the dockyard. The commissioning of the compressor was done in a relatively short period of time. One of the minor problems encountered during commissioning was high gearbox vibration, occurring at a specific speed range and resulting in several machine trips. Measurements performed by the gearbox manufacturer, with additional instrumentation, showed that these vibrations were related to local resonances of the gearbox casing. Since the high accelerometer signals were observed in a specific speed range only, it was decided to implement a higher trip value setting with a delayed initiation. This appeared to be a good practical solution.

A major problem was only encountered with the dry gas seals. Due to a failure, they both had to be replaced. The most likely cause of failure is formation of hydrocarbon condensates in the primary and secondary sealing element, which is expected to occur due to Joule-Thompson cooling prior to startup at full suction pressure of 170 barg (2465 psi). Starting at full suction pressure is beneficial, since it will reduce the downtime of a compressor trip as repressurizing is not necessary to establish forward flow. However, in order to avoid condensate due to the expansion in the seals, it was decided to start against a reduced suction pressure in the range of 21 to 25 barg (305 to 363 psi). A starting permissive indication has been implemented in the logic, in order to prevent the compressor from being started outside this pressure range.

After replacement of the dry gas seals and reduction of the starting pressure, the compressor has been in operation successfully since the end of 1998. The oil production rates of the FPSO reach 70,000 barrels per day, which is exceeding the design values by almost 40 percent. The compressor's rotordynamic behavior is stable with low vibration levels at running speed (Figure 29) measured at site earlier this year. It is obvious from this figure that no subsynchronous vibration component is present.

DISCUSSION

Around 20 years ago, a research project was executed at the company employing the two leading authors concerning the design of compressors for high-pressure applications. For this rather extensive project, a 900 bar (13,050 psi) compressor was designed, manufactured, and successfully tested at full load operating conditions (Demag, 1981). For this design, all possible measures were taken in order to ensure a stable rotor behavior. Although it was possible at that time to successfully operate this compressor, the margin to the onset of instability was not accurately known.

Nowadays, as shown with the results of the labyrinth test rig described in this paper, it has become possible to accurately establish the dynamic labyrinth seal coefficients and apply these coefficients for reliable rotor stability analyses of compressor applications.

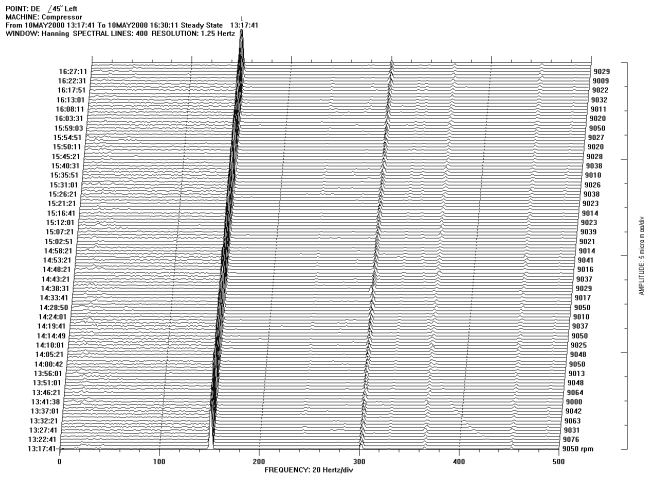

Figure 29. Vibration Spectra from the Field.

In 1999, a feasibility study was executed by the company employing the two leading authors for the application of a 1000 bar (14,500 psi) natural gas reinjection compressor. This project was initiated by a consortium of several major companies in the oil and gas business. Since this study has shown that there are certainly good prospects to successfully build and operate such a machine when taking into account various measures, the question is being raised where the limit would be. It will be an enormous challenge for the design engineers of high-pressure compressors to extend the boundaries further and tread new ground in the near future.

CONCLUSION

A general overview has been given for the design of high-pressure centrifugal compressors taking into account aspects of the casing, the impellers, the labyrinth seals, and the rotor design. A transient FEA study has been executed in order to establish the actual operating clearance of the balance drum labyrinth during startup of the unit. This analysis was successfully verified by experiments on the test stand.

Special consideration was given to the destabilizing forces of the labyrinth seals on the rotordynamic behavior. A systematic design approach for the stability of high-pressure compressors has been given. Rotor stability verification at the test stand, under actual operating conditions, confirmed the accuracy of the analytical predictions. It has been made clear again that swirl brakes do have a major positive contribution on the rotor stability.

It is the authors' opinion that a systematic and analytical design approach as shown in this paper will lead to the design of reliable compressors for very high pressure applications.

REFERENCES

Aarnink, H. J., Willemsen, T. C., and Derkink, J. G. H., 1993, "ASME PTC-10 Class I Performance Test Results Correlated with Class III Results," IMechE C449/027/93.

Aarnink, H. J., Willemsen, T. C., and Magee, J., 1999, "Dry Gas Seal Reliability Development, A Compressor Vendor Viewpoint," IMechE S620, Seminar on the Reliability of Rotating Machinery Sealing Systems.

API Standard 617, 1995, "Centrifugal Compressors for Petroleum, Chemical, and Gas Service Industries," Sixth Edition, American Petroleum Institute, Washington, D.C.

ASME PTC-10, 1997, "Compressor and Exhausters," American Society of Mechanical Engineers, New York, New York.

Azuaje, E. A. S., 1997, "Experimental Rotordynamic Coefficient Results for (a) A Labyrinth Seal With and Without Shunt Injection and (b) A Honeycomb Seal," MSc Thesis, Texas A&M University.

Baumann, U. 1999, "Rotordynamic Stability Tests on High-Pressure Radial Compressors," *Proceedings. of the Twenty-Eighth Turbomachinery Symposium*, Turbomachinery Laboratory, Texas A&M University, College Station, Texas, pp. 115-122.

Benckert, H., 1980, "Strömungsbedingte Federkennwerte in Labyrinthdichtungen," Dissertation, Universität Stuttgart.

Bromham, R. J., Lorenzen, H., and Aicher, W., 1996, "The Integration of Process and Compressor Design for a Difficult North Sea Gas Re-injection Duty," IMechE Publication C508/030/96.

Brown, R. D. and Hart, J. A., 1986, "A Novel Form of Damper for Turbomachinery," Proceedings of the First European Sponsored Turbomachinery Symposium, Brunel University, United Kingdom.

Buse, M. P., de Jongh, F. M., and Vial, F. H., 1996, "Performance Improvement of Low Volume Flow Centrifugal Compressor Stages," IMechE C508/033/96.

Campbell, W., 1924, "The Protection of Steam Turbine Disk Wheels From Axial Vibration," Transactions of the ASME, *46*, pp. 31-160.

Childs, D. W., 1993, *Turbomachinery Rotordynamics: Phenomena, Modeling, and Analysis*, New York, New York: John Wiley & Sons, Inc.

de Jongh, F. M. and Morton, P. G., 1996, "The Synchronous Instability of a Compressor Rotor Due to Bearing Journal Differential Heating," ASME Transactions, Journal of Engineering for Gas Turbines and Power, *118*, pp. 816-824.

de Jongh, F. M. and van der Hoeven, P., 1998, "Application of a Heat Barrier Sleeve to Prevent Synchronous Rotor Instability," *Proceedings of the Twenty-Seventh Turbomachinery Symposium*, Turbomachinery Laboratory, Texas A&M University, College Station, Texas, pp. 17-26.

de Jongh, F. M., Rip, F. W., and Wesselink, A. J. F., 1989, "A Full Load Test, Using a Mixture of Hydrocarbons, Performed on an Indoor Test Stand," IMechE C390/029.

Demag, 1981, "Centrifugal Compressors for Ultra-High Pressures," Company Brochure MA 25.69 en/12.81.

Fulton, J. W., 1984, "The Decision to Full Load Test a High Pressure Centrifugal Compressor in its Module Prior to Tow-Out," IMechE, Second European Congress on Fluid Machinery for the Oil, Petrochemical, and Related Industries, The Hague, The Netherlands, S. 133-138.

Gelin, A., Pugnet, J. M., Bolusset, D., and Friez, P., 1996, "Experience in Full-Load Testing Natural Gas Centrifugal Compressors for Rotordynamic Improvements," ASME 96-GT-378.

Jansen, W. and Fetfatsidis, P. K., 1999, "Fatigue Failures of Centrifugal Impeller Disks," ASME 99-GT- 427, Indianapolis, Indiana.

Kirk, R. G., April 1988, "Evaluation of Aerodynamic Instability Mechanisms for Centrifugal Compressors—Part II: Advanced Analysis," *Journal of Vibration, Acoustics, Stress, and Reliability in Design*, *110*, pp. 207-212.

Kirk, R. G. and Donald, G. H., 1983, "Design Criteria for Improved Stability of Centrifugal Compressors," Rotor Dynamical Instability, AMD, *55*, pp. 59-72.

Kleynhans, G. and Childs, D., 1996, "The Acoustic Influence of Cell Depth on the Rotordynamic Characteristics of Smooth-Rotor/Honeycomb-Stator Annular Gas Seals," Rotordynamic Instability Problems in High-Performance Turbomachinery, NASA Conf. Publ. 3344, pp. 49-76.

Kocur, J. A., and de Jongh, F. M., 2000, "Thermal Rotor Instability in Gas Compressors," Proceedings of the XIV International Gas Convention, Caracas, Venezuela.

Kocur, J. A., Platt, J. P., and Shabi, L. G., 1987, "Retrofit of Gas Lubricated Face Seals in a Centrifugal Compressor," *Proceedings of the Sixteenth Turbomachinery Symposium*, Turbomachinery Laboratory, Texas A&M University, College Station, Texas, pp. 75-84.

Kuzdzal, M. J., Hustak, J. F., and Sorokes, J. M., 1994, "Identification and Resolution of Aerodynamically Induced Subsynchronous Vibration During Hydrocarbon Testing of a 34,000 HP Centrifugal Compressor," Proceedings of the Fourth International Conference on Rotordynamics, Chicago, Illinois, IFToMM.

Memmott, E. A., 1992, "Stability of Centrifugal Compressors by Applications of Tilt Pad Seals, Damper Bearings and Shunt Holes," C432/070 IMechE.

Memmott, E. A., July 1999, "Stability Analysis and Testing of a Train of Centrifugal Compressors for High Pressure Gas Injection," *Journal of Engineering for Gas Turbines and Power*, *121*.

Millsaps, K. T. and Martinez-Sanchez, M., October 1994, "Dynamic Forces from Single Gland Labyrinth Seals: Part II – Upstream Coupling," *Journal of Turbomachinery*, *116*, pp. 694-700.

Nielsen, K. K., Childs, D. W., and Myllerup, C. M., 2000, "Experimental and Theoretical Comparison of Two Swirl Brake Designs," ASME Turbo Expo 2000, Munich, Germany, ASME 2000-GT-0399.

Nielsen, K. K., Myllerup, C. M., and van den Braembussche, R. A., 1999, "Parametric Study of the Flow in Swirl Brakes by Means of a Three-Dimensional Navier-Stokes Solver," IMechE Publication C557/088/99.

Rao, J. S., 1991, *Turbomachine Blade Vibrations*, New York, New York: John Wiley and Sons.

Sorokes, J. M., Kuzdzal, M. J., Sandberg, M. R., and Colby, G. M., 1994, "Recent Experiences in Full Load Full Pressure Shop Testing of a High Pressure Gas Injection Centrifugal Compressor," *Proceedings of the Twenty-Third Turbomachinery Symposium*, Turbomachinery Laboratory, Texas A&M University, College Station, Texas, pp. 3-18.

Srinivasan, A. V., 1997, "Flutter and Resonant Vibration Characteristics of Engine Blades," (1997 IGTI Scholar Paper), ASME Transactions, Journal of Engineering for Gas Turbines and Power, *119*, pp. 742-775.

Wagner, N. G., 1999, "Reliable Rotor Dynamic Design of High Pressure Compressors Based on Test Rig Data," ASME International Gas Turbine and Aeroengine Congress and Exhibition, Indianapolis, Indiana, ASME 99-GT-150.

Wagner, N. G. and Steff, K., 1996, "Dynamic Labyrinth Coefficients from a High-Pressure Full-Scale Test Rig Using Magnetic Bearings," Rotordynamic Instability Problems in High-Performance Turbomachinery, NASA Conf. Publ. 3344, pp. 95-112.

Wallmann, T., 2000, "Improved 2-D Impeller Family for Low Flow Coefficients," Proceedings of the Sixth International Symposium, Compressor Users—Manufacturers, Saint Petersburg, Russia (in Russian).

Wang, Q., Bartos, J. C., and Houston, R. A., 1999, "Methodology of Open Bladed Impeller Resonance Identification," *Proceedings of the Twenty-Eighth Turbomachinery*

Symposium, Turbomachinery Laboratory, Texas A&M University, College Station, Texas, pp. 61-68.

Wyssmann, H., Lorenzen, J., and Pluess, F., 1987, "Design, Testing and Commissioning of the Reinjection Centrifugal Compressors for the Alrar Gas Treatment Plant," IMechE Publication C103/87.

Zeidan, F. Y., Perez, R. X., and Stephenson, E. M., 1993, "The Use of Honeycomb Seals in Stabilizing Two Centrifugal Compressors," *Proceedings of the Twenty-Second Turbomachinery Symposium*, Turbomachinery Laboratory, Texas A&M University, College Station, Texas, pp. 3-16.

ACKNOWLEDGEMENT

The authors wish to thank the management of Demag Delaval Turbomachinery and of APS for authorizing the publication of this project. The authors also acknowledge the FEA contributions of Marcel Buse and Helmut Wirtz to this project.